Published in final edited form as:
Nature. 2018 August ; 560(7717): 192–197. doi:10.1038/s41586-018-0356-z.

Cyclin-dependent kinase 12, a novel drug target for visceral leishmaniasis

Susan Wyllie[a], **Michael Thomas**[a], **Stephen Patterson**[a], **Sabrinia Crouch**[b], **Manu De Rycker**[a], **Rhiannon Lowe**[c], **Stephanie Gresham**[c], **Michael D. Urbaniak**[a,d], **Thomas D. Otto**[e], **Laste Stojanovski**[a], **Frederick Simeons**[a], **Sujatha Manthri**[a], **Lorna M. MacLean**[a], **Fabio Zuccotto**[a], **Nadine Homeyer**[a], **Hannah Pflaumer**[f], **Markus Boesche**[f], **Lalitha Sastry**[a], **Paul Connolly**[g], **Sebastian Albrecht**[a], **Matt Berriman**[e], **Gerard Drewes**[f], **David W. Gray**[a], **Sonja Ghidelli-Disse**[f], **Susan Dixon**[h], **Jose M. Fiandor**[b], **Paul G. Wyatt**[a], **Michael A. J. Ferguson**[a], **Alan H. Fairlamb**[a], **Timothy J. Miles**[b,*], **Kevin D. Read**[a,*], and **Ian H. Gilbert**[a,*]

[a]Drug Discovery Unit, Wellcome Centre for Anti-Infectives Research, Division of Biological Chemistry and Drug Discovery, School of Life Sciences, University of Dundee, Dundee, UK

[b]Global Health R&D, GlaxoSmithKline, Calle Severo Ochoa 2, 28760, Tres Cantos, Madrid, Spain

[c]GlaxoSmithKline, David Jack Centre for R&D, Park Road, Ware, Hertfordshire, SG12 0DP, UK

[d]Division of Biomedical and Life Sciences, Faculty of Health and Medicine, Lancaster University, Lancaster LA1 4YG, UK

[e]Wellcome Sanger Institute, Hinxton, Cambridge CB10 1SA, UK

[f]Cellzome - a GlaxoSmithKline company, Meyerhofstrasse 1 69117 Heidelberg, Germany

[g]GlaxoSmithKline, New Frontiers Science Park, Third Avenue, Harlow, Essex. CM19 5AW, UK

[h]GlaxoSmithKline, Stockley Park West, West Drayton, Uxbridge, UB11 1BT, UK

Summary

Visceral leishmaniasis (VL) causes significant mortality and morbidity in many parts of the world. There is an urgent need for the development of new, effective treatments for this disease. We

Correspondence and requests for materials should be addressed to Ian Gilbert (i.h.gilbert@dundee.ac.uk), Kevin Read (k.read@dundee.ac.uk) or Tim Miles (tim.j.miles@gsk.com).

Author Contributions: these are recorded in detail in the supporting information. In brief, S.W., M.D.U., T.D.O, H.P., M.Bo., and S.M. carried out the mode of action, genomic and proteomic studies. M.T., S.P. and S.A. carried out the chemistry. M.D.R., S.M., L.M.M. and L.Sa. carried out the parasite screening. S.C., L.S., F.S., and P.C. carried out the drug metabolism and pharmacokinetic studies. F.Z and N.H. carried out the molecular modelling. R.L. and S.G. carried out the safety studies. S.W., M.T., S.P., M.D.R., R.L., S.G., M.D.U., L.M.M., F.Z., M.Be., G.D., D.W.G., S.G.-D., S.D., J.M.F., P.W.G., M.A.J.F., A.H.F., T.J.M., K.D.R., and I.H.G. designed experiments, managed parts of the project and contributed to the writing.

Author Information: Reprints and permissions information is available at www.nature.com/reprints.

The authors declare the following financial interests: these authors have shares in GlaxoSmithKline: PGW, SD, TJM, KDR, SC, RL, SG, MB, HP, PC, GD, DG, SG-D and JMF.

Data Availability. Compound **7** is currently in pre-clinical development and full disclosure of the synthesis of this compound has been included in this publication. All reasonable requests for the other key tool molecules disclosed in this manuscript will be met subject to an appropriate material transfer agreement in place between all parties.

Europe PMC Funders Author Manuscripts

describe the development of a novel anti-leishmanial drug-like chemical series based on a pyrazolopyrimidine scaffold. The leading compound from this series (**7**, **DDD853651/ GSK3186899**) is efficacious in a mouse model of VL, has suitable physicochemical, pharmacokinetic and toxicological properties for further development and has been declared a preclinical candidate. Detailed mode of action studies indicate that compounds from this series act principally by inhibiting the parasite cdc-2-related kinase 12 (CRK12), thus defining a novel, druggable, target for VL.

Introduction

Leishmania parasites cause a wide spectrum of human infections ranging from the life-threatening visceral disease to disfiguring mucosal and cutaneous forms. *Leishmania* spp. are obligate intracellular parasites of the vertebrate reticuloendothelial system, where they multiply as amastigotes within macrophage phagolysosomes; transmission is by blood-sucking sandflies, in which they proliferate as extracellular promastigotes.

Visceral leishmaniasis (VL), resulting from infection with *Leishmania donovani* and *L. infantum*, causes more than 30,000 deaths annually, of which ~60% occur in India, Bangladesh and Nepal1. In 95% of cases, death can be prevented by timely and appropriate drug therapy2. However, current treatment options are far from ideal with outcomes dependent upon a number of factors including geographical location, the immune status and other co-morbidities of the patient, and the disease classification. None of the current front-line treatments for VL, amphotericin B (liposomal or deoxycholate formulations), miltefosine, paromomycin and antimonials, are ideal for use in resource poor settings, due to issues such as teratogenicity, cost, resistance and / or clinical relapse, prolonged treatment regimens and parenteral administration3–5. Thus, there is an urgent need for new treatment options for VL, particularly oral drugs. Unfortunately, there are currently no new therapeutics in clinical development and only a few in preclinical development. There is a paucity of well-validated molecular drug targets in *Leishmania,* and the molecular targets of the current clinical molecules are unknown. Recent studies6 identified the proteasome as a promising therapeutic target for treatment of VL as well as other kinetoplastid infections, and this currently represents the most robustly validated drug target in these parasites. Furthermore, whole cell (phenotypic) screening programs have been hindered by extremely low hit rates7. Here, we report the discovery of a promising new anti-leishmanial compound with a novel mechanism of action.

Discovery

Previously, we reported the identification of a diaminothiazole series from a compound screen against *Trypanosoma brucei* GSK3 kinase (*Tb*GSK3)8. During compound optimization it became clear that the anti-trypanosomal activity of the series was driven, at least in part, by off-target activity. The early compounds showed activity against *T. brucei* bloodstream trypanosomes in viability assays, but showed little activity against *L. donovani* axenic amastigotes (e.g. compound **1**). Modification of the core structure, whilst retaining hydrogen bond donor and acceptor functionalities, gave a bicyclic compound series (Fig. 1),

Europe PMC Funders Author Manuscripts

one of which (compound **2**), showed very weak activity against *L. donovani* axenic amastigotes, but was inactive against the clinically relevant intra-macrophage amastigotes. Appending a sulfonamide to the cyclohexyl ring resulted in compound **3**, active against *L. donovani* amastigotes in both the axenic and intra-macrophage assays9,10 and selectively active against *L. donovani* compared to the THP-1 mammalian host cells used in the assay. Replacement of the *iso*-butyl substituent on the pyrazole ring with an aromatic substituent and the benzyl group on the sulfonamide with a trifluoropropyl substituent resulted in compound **4** which had marginally more activity. Critically this compound demonstrated >70% parasite reduction in a mouse model of VL when dosed orally, providing proof of concept in an animal model for this series. Replacing the pyridyl group with a 2-methoxyphenyl and the trifluoropropyl group with an *iso*-butyl group gave our most potent compound **5**, which had an EC_{50} of 0.014 μM in the intra-macrophage assay. Compound **5** was metabolically unstable, although it demonstrated >95% parasite reduction when dosed in a HRN™ hepatic CYP450 null mouse model of infection11. Furthermore, the solubility of compounds **4** and **5** was poor.

The 2-methoxyphenyl group of **5** was replaced by a morpholine (compound **6**) to increase polarity, increase the 3-dimensional shape (sp3 character) and reduce the number of aromatic rings. This was substituted with a 2-methyl group to further reduce the planarity and the trifluoropropyl sulfonamide was re-introduced, to give the key compound **DDD853651 / GSK3186899** (compound **7**)12. This compound was selected as our preclinical candidate, on the basis of the overall properties of the molecule (potency, efficacy in the mouse model, pharmacokinetics and safety profile).

Compound **7** was active against *L. donovani* in an intra-macrophage assay9 with an EC_{50} of 1.4 μM (95% Confidence Interval (CI) 1.2-1.5 μM, n=12) and showed good selectivity against mammalian THP-1 cells (EC_{50} >50 μM). This is not as potent as our reported data for amphotericin B (EC_{50} of 0.07 μM in the intra-macrophage assay), but is comparable to the clinically used drugs miltefosine and paromomycin (EC_{50} values of 0.9 μM and 6.6 μM, respectively)9. Compound **7** was also active in our cidal axenic amastigote assay (EC_{50} 0.1 μM (95% CI 0.06-0.17 μM, n=4)10. At a concentration of 0.2 μM, compound **7** was cytocidal at 96 h; increasing the concentration to 1.8 μM reduced this to 48 h (Extended Data Fig. 1). Compound **7** demonstrated a less than 10-fold variation in potency against a panel of *Leishmania* clinical-derived lines. The compound was also more active in a panel of *Leishmania* lines using human peripheral mononuclear cells as host cells (Extended Data Table 1).

A balance between solubility in relevant physiological media (Extended Data Table 2) and *in vitro* potency proved key for development of this series. Compound **7** was stable in microsomes and hepatocytes, predictive of good metabolic stability (Extended Data Table 3). The compound was orally bioavailable and showed a linearity of pharmacokinetics from 10 to 300 mg/kg in rats (Extended Data Table 4). In our mouse model of infection the compound demonstrated comparable activity to the front-line drug miltefosine, reducing parasite levels by 99% when dosed orally twice a day for 10 days at 25 mg/kg (Fig. 2). Efficacy of treatment was dependent on dose, frequency (twice a day better than once), and duration (10 days better than 5). The non-clinical safety data for s regulatory preclinical

studies. *In vitro* assays demonstrated that this compound did not significantly inhibit cytochrome P450 enzymes, mitigating a potential risk of problematic drug-drug interactions that is particularly relevant due to the frequency of VL/HIV co-infections1.

As the series was developed from a known protein kinase scaffold13, Cellzome's Kinobead™ technology was used to determine if compound **7** inhibits human protein kinases14. These experiments indicated that compound **7** interacted with four human kinases, MAPK11, NLK, MAPK14 and CDK7, at concentrations within multiples of the predicted clinical dose (Table S1). However, the extent of inhibition of these human kinases is not sufficient to preclude clinical development of the molecule and no significant inhibition of other human kinases was detected in the Kinobead™ assays. Non-GLP preclinical assessment of cardiovascular effects and genotoxicity did not reveal any issues that would prevent further development. Additionally, there were no significant adverse effects in a rat 7-day repeat dose oral toxicity study with respect to clinical chemistry and histopathology at all doses tested. Both the *in vivo* efficacy and safety profile of compound **7** support progression to definitive safety studies.

Mode of Action Studies

Elucidating the mode of action of novel chemical series can greatly benefit drug discovery campaigns15. Since there is no blueprint to establish the mode of action of bioactive small molecules16,17, several complementary methodologies were employed. Representative pyrazolopyrimidine analogues (**4, 5, 6** and **7**) from the drug discovery program were used as chemical tools (Fig. 1), including compound **8**, where the diaminocyclohexyl group was replaced by an aminopiperidine amide. These compounds showed very good activity correlation between the intra-macrophage, axenic amastigote and promastigote assays, giving us confidence to use the extracellular parasite forms (promastigote) for mode of action studies where it was not possible to use the intracellular forms (amastigote) (Table S2).

As a first step towards identifying the target(s) of the leishmanocidal pyrazolopyrimidine series, structure activity relationships were used to inform the design of analogues containing a polyethyleneglycol (PEG) linker (**9**, **11**, **12**; Extended Data Fig. 2), which were then covalently attached to magnetic beads to allow for chemical proteomics. Firstly, beads derivatized with **9** were used to pull down proteins from SILAC (Stable Isotope Labelling by Amino Acids in Cell Culture)-labelled *L. donovani* promastigote lysates18 in the presence ("light-labelled lysate") or absence ("heavy-labelled lysate") of 10 μM compound **10**, a structurally related, bioactive derivative of compound **9** 19. After combining the bead eluates and performing proteomic analyses, proteins that bound specifically to the pyrazolopyrimidine pharmacophore could be distinguished from proteins that bound non-specifically to the beads by virtue of high heavy : light tryptic peptide isotope ratios. These experiments identified CRK12, CRK6, CYC9, CRK3, MPK9, CYC6 and a putative STE11-like protein kinase (LinJ.24.1500) as specific binders to the compound **9**-derivatised beads (Log_2 heavy : light ratio >2.8; 7-fold enrichment) (Fig. S5; Table S3). Secondly, pull down experiments were conducted with beads derivatized with **9**, **11** or **12**, followed by competition studies with **5, 8** and **8**, respectively. Adherent proteins were washed off the

beads, digested with trypsin and labelled with isobaric tandem mass tags. Comparison of the labelled peptides derived from experiments, with and without competition, by liquid chromatography / mass spectrometry identified proteins likely to specifically bind to the immobilized ligands. Potential candidates identified included: CRK3, CRK6, CRK12, CYC3, CYC6, CYC9, MPK9, MPK5 and several hypothetical proteins (Fig. S6; Table S4). We also investigated immobilizing the compound at an alternate position on the scaffold and this gave a similar binding profile (Fig. S6; Table S4), further validating the approach. These results are consistent with previous studies which report that the pyrazolopyrimidine core binds to protein kinases13,20–22.

The presence of cdc2-related kinases (CRK3, 6 and 12) and cyclins (CYC3, 6 and 9) in the initial target list led us to analyze the effects of pyrazolopyrimidines (**5, 6, 7** and **8**) on cell-cycle progression in *L. donovani*. Treatment resulted in an accumulation of cells in G1 and in G2/M and a decrease in the proportion of cells in S phase (Fig. 3a for compound **7** and Fig. S9 for **5**, **6** and **8**), suggesting arrests in the cell-cycle at G1/S and G2/M, consistent with a mode of action *via* CRK and/or CYC components.

Resistance was generated in *L. donovani* promastigotes against compounds **4** and **5**. A single cloned parental cell line was divided into three individual cultures for each compound and resistance was generated by exposing parasites to step-wise increasing concentrations of compound. Following resistance generation, each independently generated cell line was cloned and 3 individual clones from each compound selection (6 in total) were selected for in depth study. The resulting clones demonstrated >500-fold and 9→17-fold resistance to compounds **4** and **5**, respectively (Extended Data Table 5). Resistance to both compounds was found to be stable over 50 days in culture in the absence of drug pressure and, significantly, all clones showed cross-resistance to **4** and **5**, and 20→50-fold cross-resistance to **7**. These data suggest our pyrazolopyrimidines share common mechanisms of resistance and most likely modes of action. Importantly, intracellular amastigotes, derived from the resistant promastigotes, were 8.5-fold and 5-fold resistant to **5** and **7**, respectively, compared to wild-type parasites (Extended Data Table 6) strongly suggesting that their mechanism(s) of action are the same in promastigote and intracellular amastigote stages of the parasite.

To gain further insight into the mechanism of action and potential target(s) of this pyrazolopyrimidine series, our 6 drug-resistant clones underwent whole genome sequence analysis. A range of mutations, relative to parental clones, were found across the genome (Table S5), including a long region with loss of heterozygosity on chromosome 9. In total, 75 sites were identified genome-wide that each had single base substitutions resulting in a non-synonymous change in at least one clone (Table S6). The majority (65) of non-synonymous substitutions consisted of derived clones losing a parental allele but amplifying the remaining allele. In five of the six resistant clones a new heterozygous substitution was selected in a single gene of unknown function (LdBPK_251630) but most strikingly, in all 6 drug-resistant clones, a single homozygous non-synonymous substitution was found in CRK12 (LdBPK_090270), a gene within the long loss-of-heterozygosity region. This mutation changes Gly572 to Asp and falls within the region predicted to encode the catalytic domain of *L. donovani* CRK12. This suggests that CRK12 is the target of the pyrazolopyrimdines. Extensive variations in chromosomal copy numbers are common in

*Leishmania*23,24, and extra copies of chromosome 9, containing the *CRK12* gene, were found in four out of six drug-resistant clones (Table S7). Additionally, three of these four clones had extra copies of chromosome 32, containing the gene for CYC9. Previous studies in *T. brucei* have established that the partner cyclin of CRK12 is CYC925. This suggests that CYC9 may be the cognate cyclin partner for *L. donovani* CRK12.

Target validation

To dissect the role of CRK12 and CYC9 in the mechanism of action and resistance of pyrazolopyrimidines a series of protein overexpression studies were undertaken in *L. donovani* promastigotes. In all cases, overexpression of putative targets was confirmed by elevated levels of transcripts in our transgenic cell lines relative to WT, as determined by qRT-PCR (Table S8).

Counter-intuitively, overexpression of wild-type CRK12 ($CRK12^{WT}$) rendered the parasites ~3-fold more sensitive to **5** (Fig. 3b). The overexpression of CYC9 alone had no effect on compound resistance, but co-overexpression of CYC9 and $CRK12^{WT}$ rendered the transgenic parasites ~3-fold resistant to compounds **5** and **7** (Fig. 3c and Table S8). Next, we looked at the mutated (Gly572 to Asp) version of CRK12 ($CRK12^{MUT}$) identified in all of our drug-resistant clones. Overexpression of $CRK12^{MUT}$ rendered the parasites ~3.4-fold resistant to **5** (Fig. 3d and Table S8) and to the preclinical lead compound **7** (Table S8), while being equally sensitive to the unrelated nitroimidazole drug fexinidazole sulfone (Table S9). Co-overexpression of $CRK12^{MUT}$ and CYC9 rendered the parasites ~6-fold resistant to compound **7** and ~8-fold resistant to compound **5**. This shift in sensitivity is considerably greater than the 3.4-fold resistance observed with parasites overexpressing $CRK12^{MUT}$ alone (Fig. 3d). Replacing a single copy of the *CRK12* gene with a drug selectable marker left parasites ~2-fold more susceptible to compound **5** than WT (Fig. 3e, Fig. S10). We were unable to directly replace both endogenous copies of the *CRK12* gene, except in the presence of an ectopic copy of the gene, suggesting that the *CRK12* gene is essential for the growth and survival of *L. donovani* (Fig. S10).

Initially, CRK3 and CRK6 were identified as credible targets based upon our collective proteomics datasets, as well as their established roles in kinetoplastid cell cycle regulation26,27. However, whole genome sequencing, qPCR (Fig. S8) and Southern blot (Fig. S7) analysis of resistant clones confirmed that mutations within, or amplification of, the CRK3 and CRK6 genes were not responsible for resistance to pyrazolopyrimidines. Direct modulation of CRK3 and CRK6 levels within *L. donovani* promastigotes, by generating overexpressing and single gene knockout parasites, did not alter drug sensitivity (Table S8). Overexpression of CRK3 and CRK6 in combination with their cognate cyclin partners CYC6 and CYC3 was not possible since co-overexpression proved toxic. Collectively, these data suggest that the primary mechanism of action of this compound series is unlikely to be *via* CRK3 or CRK6 inhibition.

Commonly, overexpression of a compound's molecular target is accompanied by an increase in drug resistance. With this in mind, our collective data strongly suggest that the principal target of our pyrazolopyrimidine series is the CYC9-activated form of CRK12, such that overexpression of CRK12 and CYC9 together provides resistance. This hypothesis is also

consistent with the amplification of both *CRK12* and *CYC9* in resistant parasites; as well as the identification of both proteins in our SILAC and Kinobead™ proteomic datasets. That overexpression of CYC9 alone has no effect suggests that CYC9 is, to some extent, in excess over CRK12 and thus overexpression of $CRK12^{MUT}$ can provide (~3-fold) resistance that is increased when additional CYC9 is co-expressed (~8-fold). The "hyper-sensitivity" of parasites overexpressing $CRK12^{WT}$ alone to these compounds remains perplexing. One potential explanation is that $CRK12^{WT}$ bound to a pyrazolopyrimidine in the absence of a CYC9 subunit is particularly toxic to the parasite. Alternatively, elevated levels of CRK12 may well sequester other cyclins thereby preventing their essential interactions with other CRKs. Further studies will be required to test these hypotheses.

Given that the compounds from this chemical series interacted with protein kinases, in particular CRK12, we used Cellzome's Kinobead™ technology14,28,29 with axenic amastigote extracts to identify pyrazolopyrimidine-binders in the *Leishmania* kinome. These experiments were performed in the presence or absence of an excess of the soluble parent compound **5**. All proteins captured by the beads were quantified by TMT tagging of tryptic peptides followed by LC-MS/MS analysis30. CRK12, MPK9, CRK6 and CYC3 (Fig. 4a) were identified, consistent with the other experiments above. A dose response experiment was performed in which **5** was added over a range of concentrations in order to establish a competition-binding curve and determine a half-maximal inhibition (IC_{50}) value (Fig. 4b). The IC_{50} values obtained in these experiments represent a measure of target affinity, but are also affected by the affinity of the target for the bead-immobilized ligands. The latter effect can be deduced by determining the depletion of the target proteins by the beads, such that apparent dissociation constants (K_d^{app}) can be determined that are largely independent from the bead ligand30. The apparent dissociation constants (K_d^{app}) were determined as 1.4 nM for CRK12, 45 nM for MPK9, 58 nM for CYC3 and 97 nM for CRK6. These values are determined in physiological conditions (substrates, cyclins and ATP) and provide further compelling evidence that the principal target of this compound series is CRK12. Further pull-downs with a resin-bound pyrazolopyrimidine analogue (**11**) were conducted in parallel with the Kinobead™ experiments and returned broadly similar results (Fig. 4 c, d).

Collectively, our data provides strong evidence that CRK12 forms a significant interaction with CYC9: (a) our studies indicate that overexpression of CYC9 alongside CRK12 markedly increases resistance to our pyrazolopyrimidine compounds; (b) in several of our compound-resistant cell lines, additional copies of chromosome 32, containing the CYC9 gene were found; (c) in the related organism *T. brucei* CYC9 was confirmed as the partner cyclin for CRK12; (d) in several chemical proteomics studies CYC9 was identified as binding to immobilized compounds from our pyrazolopyrimidines alongside CRK12.

Modelling

A homology model was built for *L. donovani* CRK12 using the structure of human cyclin dependent kinase 9 (CDK9, PDB code:4BCF) as a template. (Interestingly **7** showed an IC_{50} > 20 μM against CDK9 in the Kinobeads™ assay.) A combination of docking studies, molecular dynamics simulation and free energy calculations indicated the most likely binding mode is that shown in Fig. 5 (see supporting information for discussion). With very

few exceptions, the binding modes of protein kinase inhibitors are highly conserved across kinase family members; searching the protein database revealed a related 5-amino-pyrazolopyrimidine, which bound to ALK in a very similar fashion (PDB code 4Z55, ligand 4LO). In our proposed binding mode, the bicyclic scaffold interacts with the hinge residues establishing two hydrogen bonds between the sp2 pyrimidine nitrogen in position 6 and the backbone NH of Ala566 and between the pyrazole NH in position 1 and the backbone carbonyl oxygen of Ala564 (Fig. 5b). A third hydrogen bond is also established between the amino NH in position 5 and the backbone carbonyl oxygen of Ala566. The substituent in position 3 of the pyrazole ring is directed towards the ATP back pocket interfacing with the gatekeeper residue (Phe563). This binding mode is consistent with the analogues **9**, **11** and **12** retaining binding affinity, with the PEG linkers being attached to water-accessible parts of the core. The Gly572Asp mutation causing resistance to the pyrazolopyrimidine series is located at the end of the hinge region nine residues from the gatekeeper. In the Gly572Asp mutant, the negatively charged side chain of the aspartic acid is positioned in close contact to the oxygen atoms of the sulfonamide moiety leading to an unfavorable electrostatic interaction.

Discussion

New oral drugs for VL, particularly those capable of treating on-going outbreaks in East Africa, are urgently needed. Effective drugs will make a significant difference to treatment outcomes for this devastating parasitic disease. With the ultimate goal of VL elimination, multiple new treatment options will be required. We have identified a pyrazolopyrimidine series showing potential to treat VL. Our studies indicate that the principal mechanism of action of our pyrazolopyrimidine compounds is through inhibition of CRK12, defining CRK12 as one of very few chemically-validated drug targets in *Leishmania*. Further, our data indicate that CYC9 is the definitive partner cyclin for CRK12. The physiological function(s) of CRK12/CYC9 have yet to be determined and the availability of our inhibitory pyrazolopyrimidines should assist in probing this aspect of parasite biology.

It is clear from our collective chemical proteomics studies that the pyrazolopyrimidines also interact with other *Leishmania* protein kinases, in particular CRK6 and CRK3, albeit with significantly lower affinities than for CRK12. While CRK12 is undoubtedly the principal target of this compound series, we cannot rule out the possibility that underlying this mechanism of action is an element of polypharmacology. Indeed, inhibition of secondary kinase targets may be responsible for some of the phenotypic effects observed in drug-treated parasites, such as cell cycle arrest.

Compound **7** is being advanced towards human clinical trials and is currently undergoing preclinical development. The data generated to date provides a reason to believe that compound **7** has the potential to fulfil the community target product profile31. However, as a systematic approach to drug discovery is relatively new in this neglected disease and there is a lack of correlation between pre-clinical and clinical data, there are outstanding questions that can only be answered as the compound progresses through development.

Europe PMC Funders Author Manuscripts

Extended Data

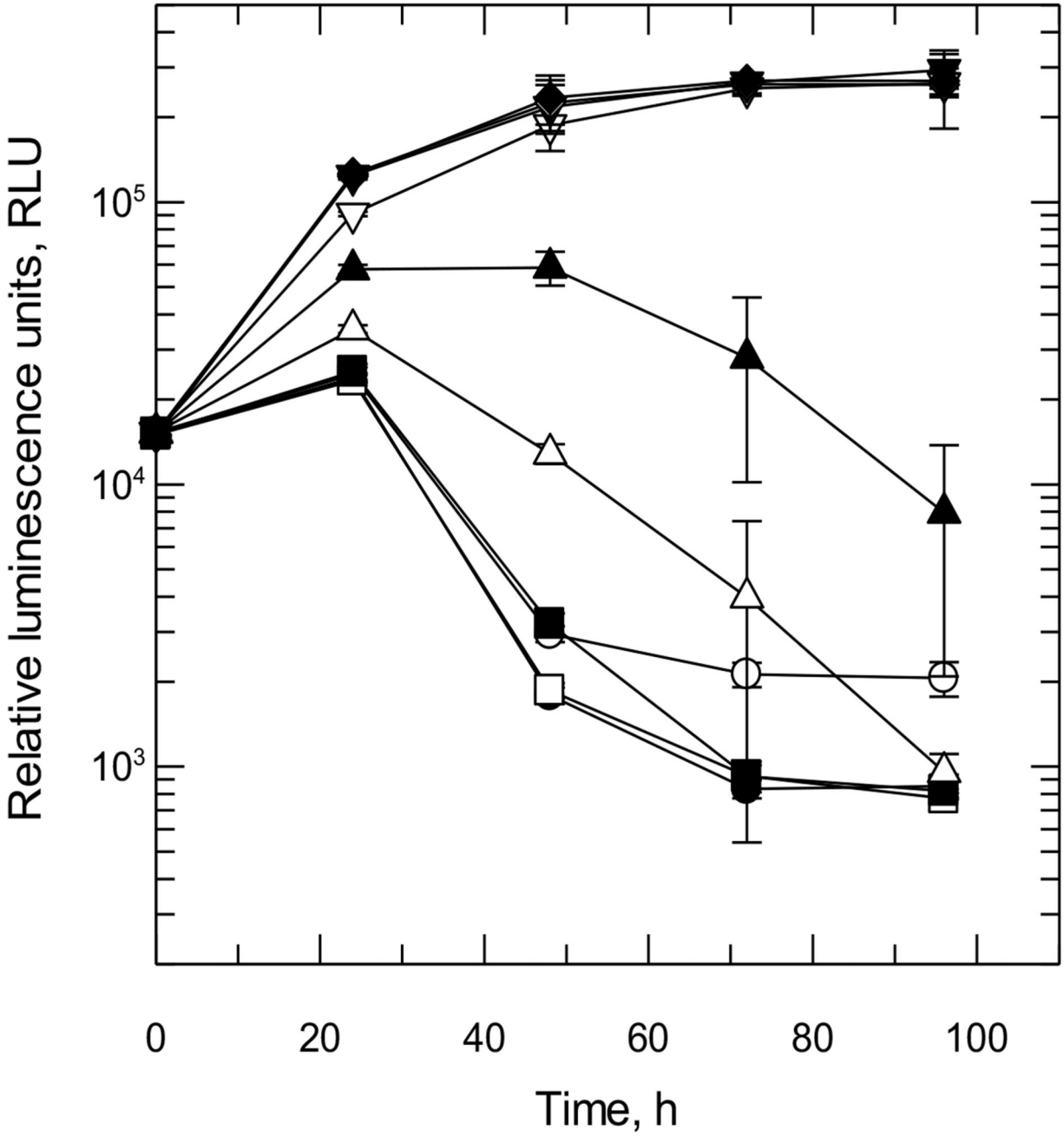

Extended Data Figure 1.

Rate-of-kill of *L. donovani* axenic amastigotes by compound **7**. Chart shows relative luminescence units (RLU) versus time from axenic amastigote rate-of-kill experiment with compound **7** (representative results for one of two independent experiments are shown; data is presented as mean and standard deviation of 3 technical replicates.). Concentrations are as follows (μM): 50, open circles; 16.7, closed circles; 5.6, open squares; 1.85, closed squares;

0.62, open triangles; 0.21, closed triangles; 0.069, open inverted triangles; 0.023, closed inverted triangles, 0.0076, open diamond and 0.0025, closed diamond.

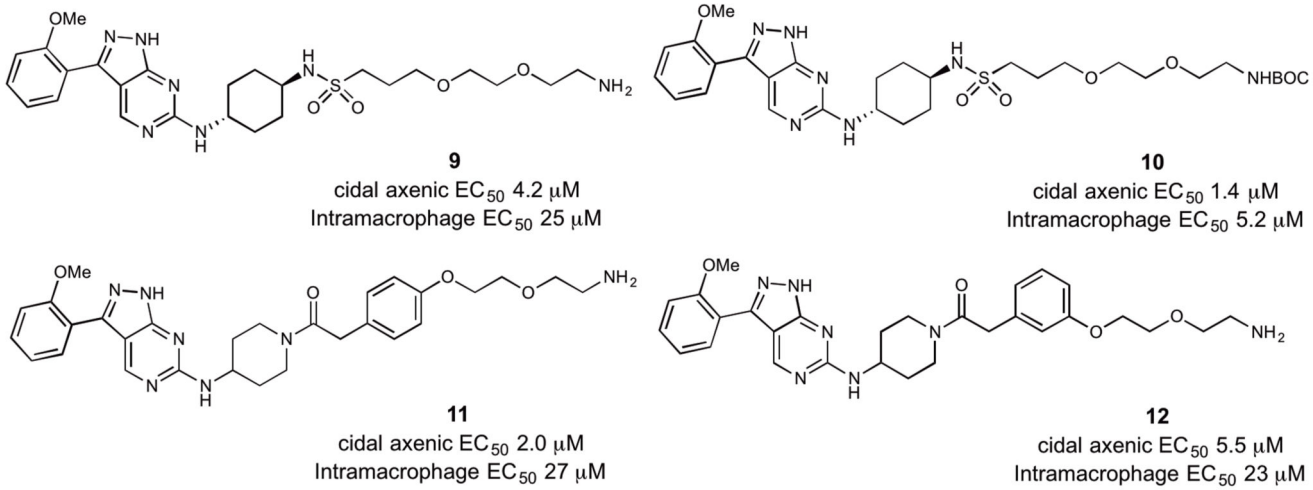

Extended Data Figure 2.
Linker-containing target molecules synthesized for chemical proteomic experiments and corresponding EC_{50} values.

Extended Data Table 1

Activity of compound 7 and miltefosine against a panel of *Leishmania* clinical isolates (intramacrophage assay using human peripheral blood mononuclear cells).

Strain	Country of origin	Year	Compound 7 EC_{50} (μM)	Miltefosine EC_{50} (μM)
L. donovani LV9	Ethiopia	1967	0.05, 0.09	0.36, 0.43
L. donovani SUKA 001	Sudan	2010	0.09	0.91
L. donovani BHUl *	India	2002	0.11	0.50
L. donovani DD8	India	1980	0.13	0.51
L. infantum ITMAP263	Morocco	1967	0.50, 0.13	1.0, 0.79

* Antimony-resistant reference strain

Strains were tested as technical duplicates on a single (DD8, SUKA001, BHU1) or two (LV9, ITMAP263) occasions; the respective EC_{50} values are shown for LV9 and ITMAP263.

Extended Data Table 2

Solubility of compound 7 in simulated physiological media (4h at 37°C).

Media	Final pH	Solubility [mg/mL]
SGF pHl.6	SGF (1.5)	1.12
Fasted SIF pH6.5	FaSSIF (6.5)	0.017
Fed SIF pH6.5	FeSSIF (6.5)	0.025

SGF, Simulated Gastric Fluid; SIF, Simulated Intestinal Fluid. Data for polyform 1.

Europe PMC Funders Author Manuscripts

Extended Data Table 3
In vitro metabolic stability data for compound 7.

Species	Concentration (μM)	Microsomes Cli (mL/min/g tissue)	Hepatocytes Cli (mL/min/g tissue)
Mouse	0.5	0.52	0.84
Rat	0.5	<0.5	0.77
Dog	0.5	<0.4	0.31
Human	0.5	0.71	0.5

Extended Data Table 4
DMPK data for compound 7

Intravenous	Mouse (male, CD1)	Rat (male, SD)
	1 mg/kg	1 mg/kg
Cl (ml/min/kg)	169 ± 50	14 ± 9
V_{dss} (L/kg)	4.0 ± 0.5	0.4 ± 0.1
$T_{1/2}$ (h)	0.3 ± 0.04	0.4 ± 0.2
$AUC_{(0\text{-}inf)}$ (ng.h/mL)	104 ± 26	1514 ± 782
Oral	10 mg/kg	10 mg/kg
C_{max} (ng/ml)	561 ± 148	1043 ± 261
T_{max} (h)	2	2
$AUC_{(0\text{-}inf)}$ (ng.h/mL)	1463 ± 362	6475 ± 2494
F% based on $AUC_{(0\text{-}inf)}$	>100	46 ±18
Oral	100 mg/kg	100 mg/kg
C_{max} (ng/ml)	8813 ± 1966	8470 ± 3750
T_{max} (h)	3	7.3
$AUC_{(0\text{-}inf)}$ (ng.h/mL)	39433 ± 23830	61202 ± 23591
F% based on $AUC_{(0\text{-}inf)}$	>100	40 ± 15
Oral	300 mg/kg	300 mg/kg
C_{max} (ng/ml)	11393 ± 4212	14833 ± 2676
T_{max} (h)	5	7.3
$AUC_{(0\text{-}inf)}$ (ng.h/mL)	*66150 ± 636	136333 ± 24846
F% based on $AUC_{(0\text{-}inf)}$	>100	51 ± 22

Extended Data Table 5

Sensitivity of WT and drug-resistant promastigotes to compounds within the series. Resistance was generated against compounds 4 and 5

Cell line	4		5		7	
	pEC_{50} (SD)	Fold	pEC_{50} (SD)	Fold	pEC_{50} (SD)	Fold
Wild type (Start clone)	7 (0.1)	1	8.2 (0.4)	1	7.1 (0.3)	1
Wild type (Age-matched)	7.1 (0.2)	1	8.2 (0.1)	1	7.3 (0.2)	1
4-resistant clone 1	< 4.3	>500	7.2 (0.1)	11	5.8 (0.4)	20
4-resistant clone 2	< 4.3	>500	7.3 (0.1)	7	5.7 (0.2)	24
4-resistant clone 3	< 4.3	>500	7 (0.2)	17	5.4 (0.1)	48
5-resistant clone l	< 4.3	>500	7.1 (0.2)	11	5.5 (0.2)	41
5-resistant clone 2	< 4.3	>500	7.1 (0.2)	14	5.5 (0.1)	35
5-resistant clone 3	< 4.3	>500	7.3 (0.1)	9	5.7 (0.1)	22

Extended Data Table 6

Sensitivity of WT and compound 5-resistant intramacrophage amastigotes (INMAC) to the compound series.

Compound	Cell line	pEC_{50}	Host cell pEC_{50}	Fold difference
5	WT	7.5	<5.3	-
5	**5** RES clone 1	6.6	<5.3	8.5
7	WT	5.9	<4.3	-
7	**5** RES clone l	5.2	<4.3	5.0

Supplementary Material

Refer to Web version on PubMed Central for supplementary material.

Acknowledgments

The authors acknowledge the Wellcome Trust for funding (grants, 092340, 105021, 100476, 101842, 079838, 098051).

References

1. Alvar J, et al. Leishmaniasis worldwide and global estimates of its incidence. PloS One. 2012; 7
2. Ritmeijer K, Davidson RN. Royal Society of Tropical Medicine and Hygiene joint meeting with Medecins Sans Frontieres at Manson House, London, 20 March 2003: field research in humanitarian medical programmes. Medecins Sans Frontieres interventions against kala-azar in the Sudan, 1989-2003. Trans R Soc Trop Med Hyg. 2003; 97:609–613. [PubMed: 16134257]

3. Sundar S, et al. Efficacy of miltefosine in the treatment of visceral leishmaniasis in India after a decade of use. Clin Infect Dis. 2012; 55:543–550. [PubMed: 22573856]
4. den Boer ML, Alvar J, Davidson RN, Ritmeijer K, Balasegaram M. Developments in the treatment of visceral leishmaniasis. Expert Opin Emerg Drugs. 2009; 14:395–410. [PubMed: 19708817]
5. Mueller M, et al. Unresponsiveness to AmBisome in some Sudanese patients with kala-azar. Trans R Soc Trop Med Hyg. 2007; 101:19–24. [PubMed: 16730363]
6. Khare S, et al. Proteasome inhibition for treatment of leishmaniasis, Chagas disease and sleeping sickness. Nature. 2016; 537:229–233. [PubMed: 27501246]
7. Don R, Ioset J-R. Screening strategies to identify new chemical diversity for drug development to treat kinetoplastid infections. Parasitology. 2014; 141:140–146. [PubMed: 23985066]
8. Woodland A, et al. From on-target to off-target activity: identification and optimisation of *Trypanosoma brucei* GSK3 inhibitors and their characterisation as anti-*Trypanosoma brucei* drug discovery lead molecules. ChemMedChem. 2013; 8:1127–1137. [PubMed: 23776181]
9. De Rycker M, et al. Comparison of a high-throughput high-content intracellular *Leishmania donovani* assay with an axenic amastigote assay. Antimicrob Agents Chemother. 2013; 57:2913–2922. [PubMed: 23571538]
10. Nuhs A, et al. Development and validation of a novel *Leishmania donovani* screening cascade for High-Throughput screening using a novel axenic assay with high predictivity of leishmanicidal intracellular activity. PLoS Negl Trop Dis. 2015; 9
11. Henderson CJ, Pass GJ, Wolf CR. The hepatic cytochrome P450 reductase null mouse as a tool to identify a successful candidate entity. Toxicol Lett. 2006; 162:111–117. [PubMed: 16343823]
12. Miles, TJ; Thomas, MG. Pyrazolo[3,4-d]pyrimidin derivative and its use for the treatment of leishmaniasis. 2016. WO 2016116563 A1 20160728
13. Ding, Q; Jiang, N; Roberts, JL. Preparation of pyrazolopyrimidines as antitumor agents. 2005. WO 2005121107
14. Bantscheff M, et al. Quantitative chemical proteomics reveals mechanisms of action of clinical ABL kinase inhibitors. Nat Biotechnol. 2007; 25:1035–1044. [PubMed: 17721511]
15. Terstappen GC, Schlupen C, Raggiaschi R, Gaviraghi G. Target deconvolution strategies in drug discovery. Nat Rev Drug Discov. 2007; 6:891–903. [PubMed: 17917669]
16. Park J, Koh M, Park SB. From noncovalent to covalent bonds: a paradigm shift in target protein identification. Mol Biosyst. 2013; 9:544–550. [PubMed: 23354063]
17. Lee H, Lee JW. Target identification for biologically active small molecules using chemical biology approaches. Arch Pharm Res. 2016; 39:1193–1201. [PubMed: 27387321]
18. Ursu A, Waldmann H. Hide and seek: Identification and confirmation of small molecule protein targets. Bioorg Med Chem Lett. 2015; 25:3079–3086. [PubMed: 26115575]
19. Urbaniak MD, Guther MLS, Ferguson MAJ. Comparative SILAC proteomic analysis of *Trypanosoma brucei* bloodstream and procyclic lifecycle stages. PloS One. 2012; 7
20. Liu Y, Gray NS. Rational design of inhibitors that bind to inactive kinase conformations. Nat Chem Biol. 2006; 2:358–364. [PubMed: 16783341]
21. Zhang L, et al. Design, synthesis, and biological evaluation of pyrazolopyrimidine-sulfonamides as potent multiple-mitotic kinase (MMK) inhibitors (part I). Bioorg Med Chem Lett. 2011; 21:5633–5637. [PubMed: 21798738]
22. Freyne, EJE; , et al. Pyrazolopyrimidines as cell cycle kinase inhibitors. 2006. WO2006074984
23. Rogers MB, et al. Chromosome and gene copy number variation allow major structural change between species and strains of *Leishmania*. Genome Res. 2011; 21:2129–2142. [PubMed: 22038252]
24. Downing T, et al. Whole genome sequencing of multiple *Leishmania donovani* clinical isolates provides insights into population structure and mechanisms of drug resistance. Genome Res. 2011; 21:2143–2156. [PubMed: 22038251]
25. Monnerat S, et al. Identification and functional characterisation of CRK12:CYC9, a novel Cyclin-Dependent Kinase (CDK)-Cyclin complex in *Trypanosoma brucei*. PloS One. 2013; 8

26. Hassan P, Fergusson D, Grant KM, Mottram JC. The CRK3 protein kinase is essential for cell cycle progression of *Leishmania mexicana*. Mol Biochem Parasitol. 2001; 113:189–198. [PubMed: 11295173]
27. Tu X, Wang CC. Pairwise knockdowns of cdc2-related kinases (CRKs) in *Trypanosoma brucei* identified the CRKs for G1/S and G2/M transitions and demonstrated distinctive cytokinetic regulations between two developmental stages of the organism. Eukaryot Cell. 2005; 4:755–764. [PubMed: 15821135]
28. Medard G, et al. Optimized chemical proteomics assay for kinase inhibitor profiling. J Proteome Res. 2015; 14:1574–1586. [PubMed: 25660469]
29. Bergamini G, et al. A selective inhibitor reveals PI3Kgamma dependence of T(H)17 cell differentiation. Nat Chem Biol. 2012; 8:576–582. [PubMed: 22544264]
30. Bantscheff M, et al. Chemoproteomics profiling of HDAC inhibitors reveals selective targeting of HDAC complexes. Nat Biotechnol. 2011; 29:255–265. [PubMed: 21258344]
31. https://www.dndi.org/diseases-projects/leishmaniasis/tpp-vl/
32. Seifert K, Croft SL. In vitro and in vivo interactions between miltefosine and other anti-leishmanial drugs. Antimicrob Agents Chemother. 2006; 50:73–79. [PubMed: 16377670]
33. Escobar P, Yardley V, Croft SL. Activities of hexadecylphosphocholine (miltefosine), AmBisome, and sodium stibogluconate (Pentostam) against *Leishmania donovani* in immunodeficient SCID mice. Antimicrob Agents Chemother. 2001; 45:1872–1875. [PubMed: 11353640]
34. Bradley DJ, Kirkley J. Regulation of *Leishmania* populations within host.1. Variable course of *Leishmania donovani* infections in mice. Clin Exp Immunol. 1977; 30:119–129. [PubMed: 606433]
35. Croft SL, Snowdon D, Yardley V. The activities of four anticancer alkyllysophospholipids against *Leishmania donovani, Trypanosoma cruzi* and *Trypanosoma brucei*. J Antimicrob Chemother. 1996; 38:1041–1047. [PubMed: 9023651]

Europe PMC Funders Author Manuscripts

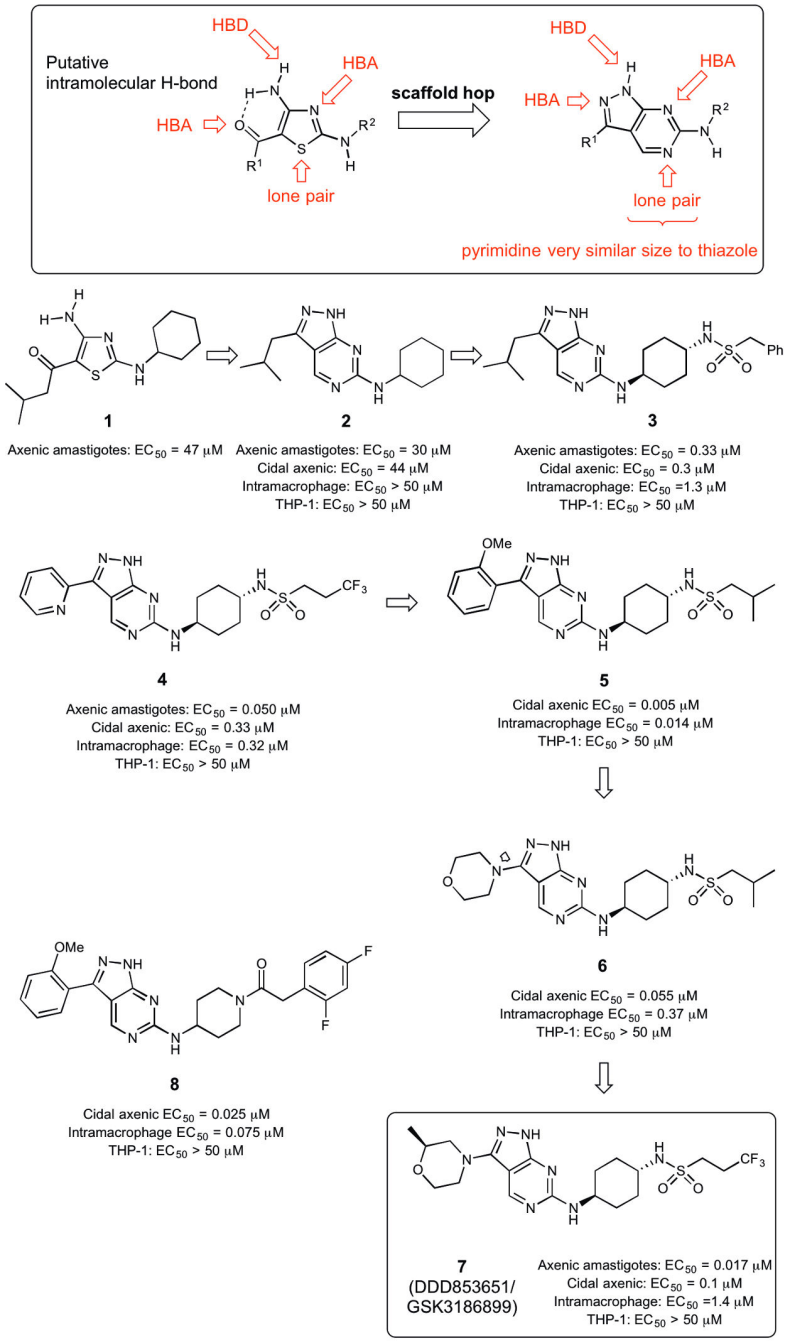

Figure 1.

The evolution of the pyrazolopyrimidine series to give the development compound **79**. Potencies against axenic amastigotes, intra-macrophage amastigotes and against THP-1 cells are shown9; data from ≥ 3 independent replicates for cidal axenic and intra-macrophage assays. In the cidal axenic assay a higher cell density and improved detection limit is used than in compared to the axenic assay allowing distinction between cytostatic and cytotoxic compounds 10.

a

Experiment no.	Dose (mg/kg)	Frequency of treatment (days)	Treatment duration (days)	Reduction in parasite load (%)	LDU[#] units in control animals
1	50	bid	5	96	370,000
2	25	bid	10	99	610,000
3	10	bid	10	49	500,000
3	3	bid	10	4	500,000
3	25	uid	5	50	570,000
4	25	uid	10	89	630,000
5	50	uid	10	95	370,000

b

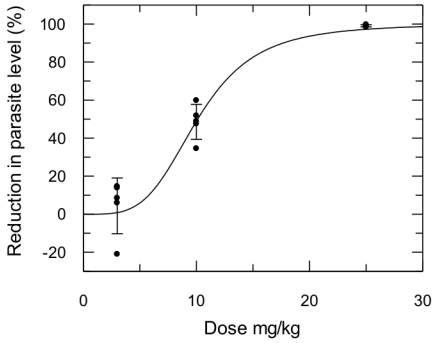

c

Suppression of Parasite Load (%)	Effective Dose (mg/kg)	95% Confidence Intervals
50	10.1	9.2 to 11.1
90	17.7	16.1 to 19.4
95	21.4	19.5 to 23.5
99	32.5	29.6 to 35.7

Figure 2.

Efficacy of compound 7 in a mouse model of VL. Each arm was carried out with 5 mice. **(a)** Reduction in parasite load for various dose regimens. uid is once daily dosing; bid is twice daily dosing. **(b)** Dose response for twice daily dosing for 10 days. **(c)** Given dose required to give a particular reduction in parasite load for twice daily dosing for 10 days. The reported ED_{90} for miltefosine in a mouse model is 27 mg/kg uid 6,32,33.

Leishman Donovan Units (LDU) are the number of amastigotes per 500 nucleated cells multiplied by the organ weight in grammes34,35.

Europe PMC Funders Author Manuscripts

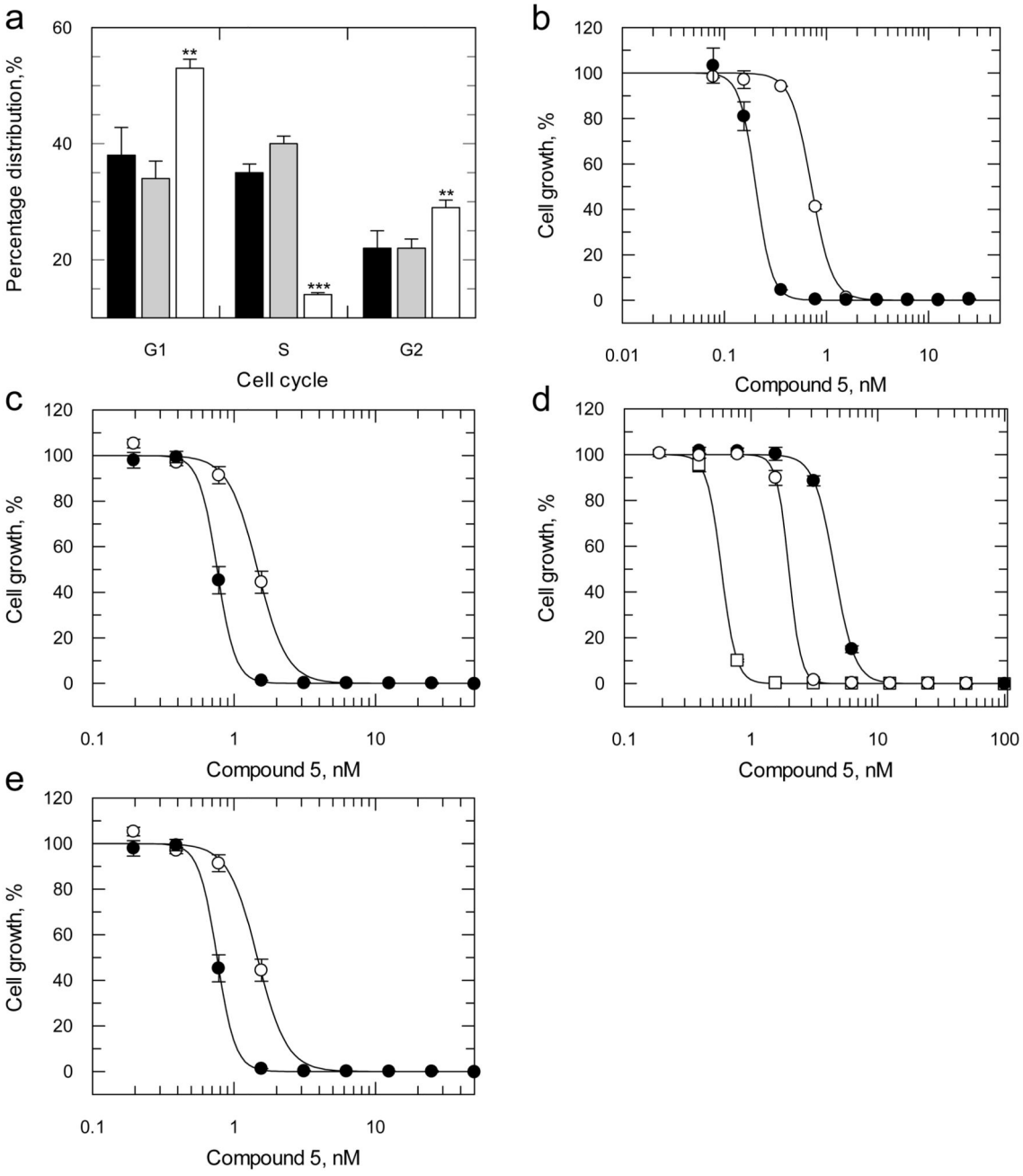

Figure 3.

Studies to validate the molecular target of the pyrazolopyrimidine series. (a) Cell cycle analysis following treatment with compounds for 8 h. Untreated cells at 0 h (black) and at 8 h (grey). Cells treated with 5x EC_{50} value of compound **7** for 8 h (white). Unpaired Student t test (**, P = 0.01; ***, P = 0.001 **(b)** Effects of $CRK12^{WT}$ overexpression in promastigotes on the potency of compound **5** (EC_{50} value of 0.24 ± 0.002 nM, closed circles) compared to WT cells (0.72 ± 0.01 nM, open circles). **(c)** Effects of $CRK12^{WT}$ and CYC9 co-overexpression in promastigotes on the potency of compound **5** (EC_{50} value of 1.43 ± 0.01

nM, closed circles) compared to WT cells (EC_{50} value of 0.5 ± 0.004 nM, open circles). **(d)** Effects of $CRK12^{MUT}$ and CYC9 overexpression in promastigotes on the potency of compound **5** (EC_{50} value of 1.99 ± 0.002 nM, open circles) compared to WT cells (EC_{50} value of 0.59 ± 0.001 nM open squares) and $CRK12^{MUT}$/CYC9 co-overexpressing promastigotes (EC_{50} value of 4.6 ± 0.05 nM, closed circles). **(e)** Effect of knocking out a single copy of the *CRK12* gene on the potency of compound **5** in promastigotes (EC_{50} value of 0.76 ± 0.004 nM, closed circles) compared to WT cells (EC_{50} value of 1.5 ± 0.004 nM, open circles). $P = 0.0014$ using an unpaired Student t test. All data are the mean ± SD from $n = 3$ technical replicates and are representative of at least duplicate experiments.

Europe PMC Funders Author Manuscripts

Europe PMC Funders Author Manuscripts

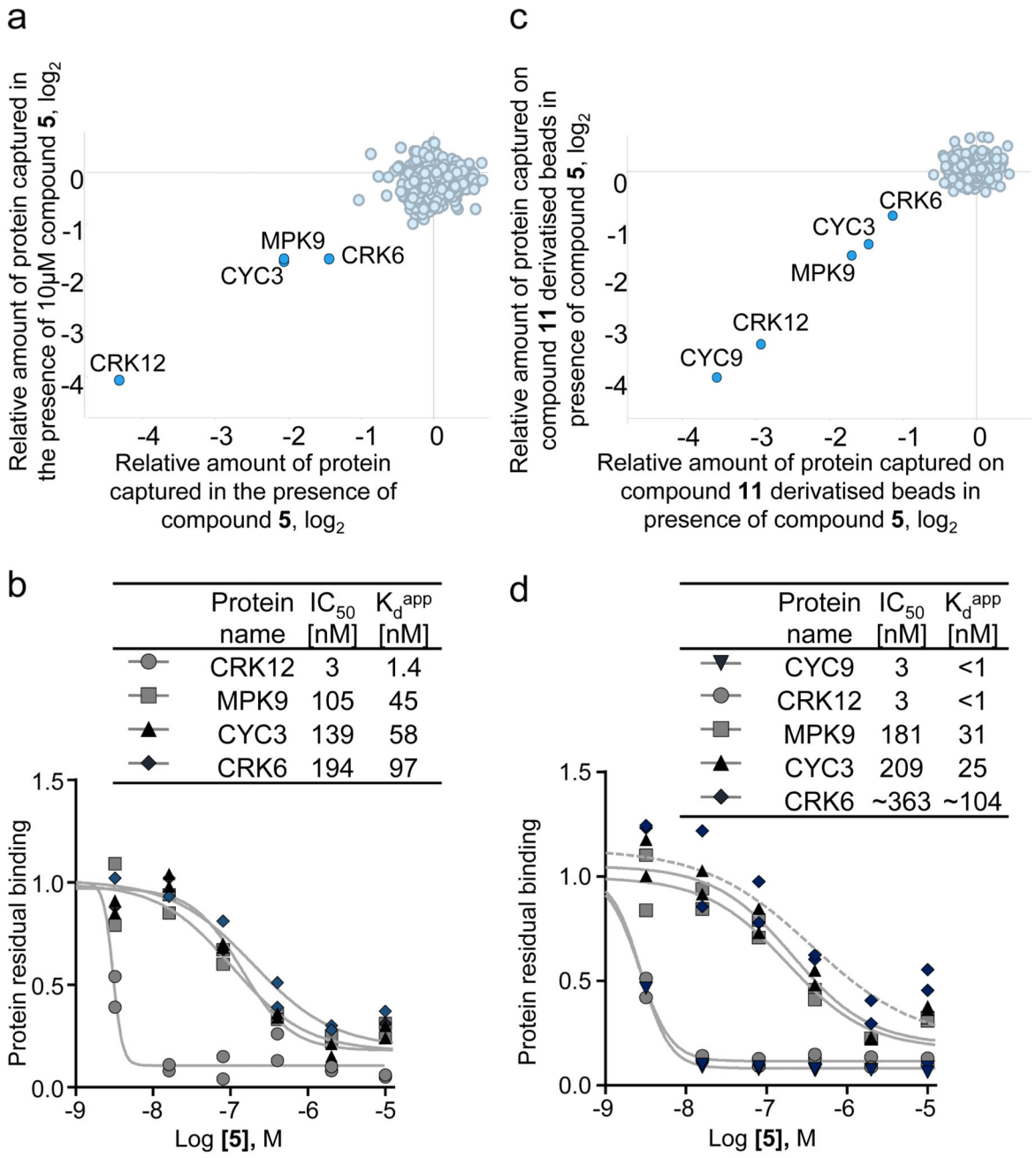

Figure 4.

Identification of cyclin dependent related kinases as targets of the pyrazolopyrimidine series using a chemoproteomic approach. (a) Relative amounts of protein captured on Kinobeads™ in the presence of 10 μM compound **5** compared to vehicle, comparison of 2 experiments. A $\log_2$ scale is used. **(b)** Dose response curves of proteins binding to Kinobeads™ in the presence of varying concentrations of compound **5**. **(c)** Relative amounts of protein captured on **11**-derviatised beads in the presence of 10 μM compound **5** compared

to vehicle, comparison of 2 experiments. A $\log_2$ scale is used. **(d)** Dose response curves of binding of proteins to **11**-derivatised beads in the presence of varying concentrations of **5**.

Europe PMC Funders Author Manuscripts

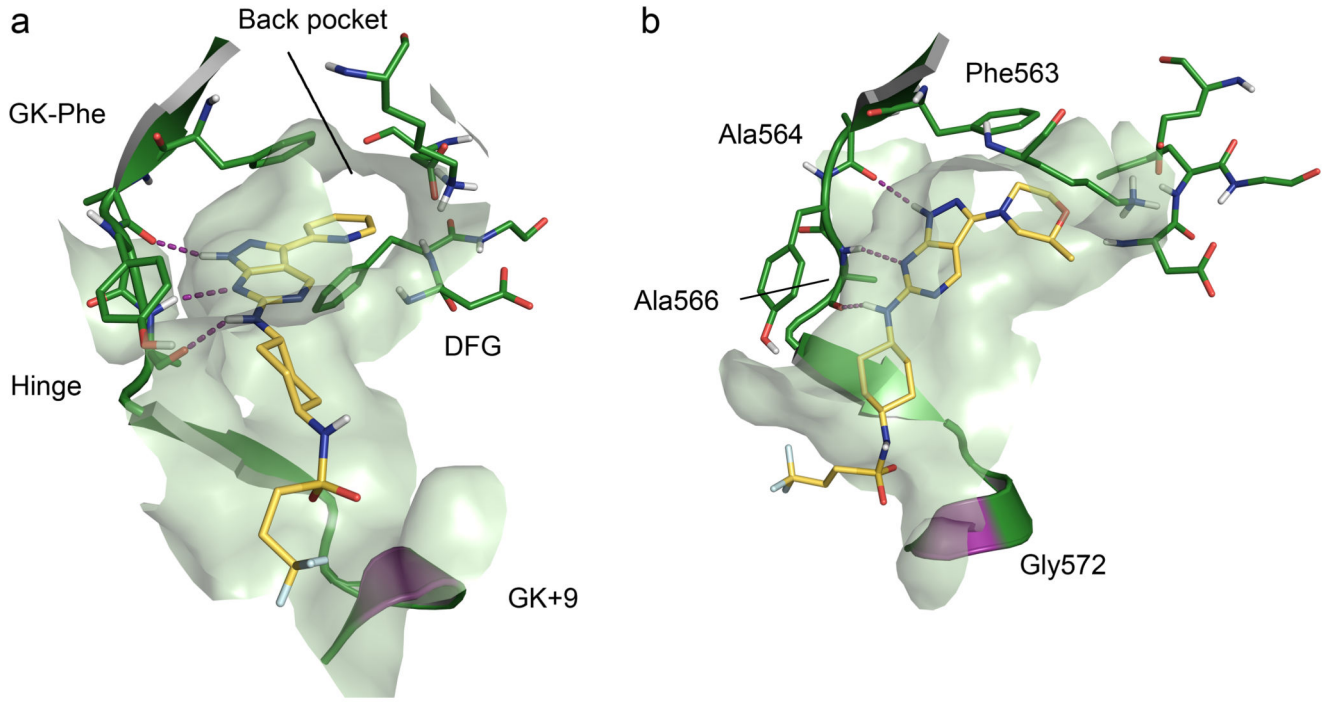

Figure 5.

Docking poses for (a) compound 4 and (b) compound 7. Dotted purple lines represent H-bonds. The mutated residue in position gate-keeper (GK) +9 is indicated in purple in the ribbon diagram.

Europe PMC Funders Author Manuscripts